Computational and Theoretical Chemistry 1237 (2024) 114648

Contents lists available at ScienceDirect

Computational and Theoretical Chemistry

journal homepage: www.elsevier.com/locate/comptc

A comparative electronic structure analysis of reactive metabolites of oxicams

Joydeep Burman [a], Kanika Manchanda [a], Kaushikkumar A. Bhakhar [a], Akshay N. Boharupi [a], Holger Gohlke [b,c], Prasad V. Bharatam [a,d,*]

[a] Department of Pharmacoinformatics, National Institute of Pharmaceutical Education and Research (NIPER), Sector-67, S.A.S. Nagar (Mohali), 160062 Punjab, India
[b] Mathematisch-Naturwissenschaftliche Fakultät, Institut für Pharmazeutische und Medizinische Chemie, Heinrich-Heine-Universität Düsseldorf, 40225 Düsseldorf, Germany
[c] Institute of Bio- and Geosciences (IBG-4: Bioinformatics), Forschungszentrum Jülich GmbH, Wilhelm-Johnen-Straße, 52425 Jülich, Germany
[d] Department of Medicinal Chemistry, National Institute of Pharmaceutical Education and Research (NIPER), Sector-67, S.A.S. Nagar (Mohali), 160062 Punjab, India

ARTICLE INFO

Keywords:
Oxicams
Reactive Metabolites
Isomers
DFT
Electrophilicity index

ABSTRACT

Oxicams are important drugs that act as anti-inflammatory agents, of them, piroxicam and its prodrugs are in daily use. The metabolic profiles of oxicams were explored using mass spectrometry methods and, in some cases, NMR. However, there is a noticeable gap in research regarding the in-depth exploration of the electronic structure of their reactive metabolites. The relative energies of the various metabolites of oxicams and the associated possible isomers have not been compared. In this work, the electronic characteristics of the reactive metabolites associated with important oxicams have been evaluated. This comparative analysis helped in identifying additional potential reactive metabolites of several oxicams. For example, the quinonimine metabolite of piroxicam has been suggested as an important possibility. This work highlights that in addition to mass spectrometry analysis, energy comparison of possible isomers needs to be carried out in drug metabolism studies.

1. Introduction

Oxicams belong to an important class of NSAIDs (Non-Steroidal Anti-Inflammatory Drugs) that exhibit anti-inflammatory effects. Though these compounds are relatively old, a lot of focused research is in progress on their mechanism of drug action [1–5]. Piroxicam, sudoxicam, meloxicam, tenoxicam, isoxicam, and lornoxicam are important drugs that exhibit anti-inflammatory, analgesic, and antioxidant activities [6]. Oxicams are used for the treatment of rheumatoid arthritis and gout [7]. They act as non-selective COX inhibitors and bind to COX-1 and COX-2 enzymes. The anticancer activity of oxicams and their metal complexes have also been reported [7]. The reactivity of the sulfonamide group in oxicams arises from the non-hypervalent nature of the sulfur atom [8]. They are weakly acidic because of the enolic-OH group present in most of them [9]. Oxicams are very much prone to form cocrystals with dicarboxylic acids which have been shown in several papers by performing synthetic and structural analysis on them [10–13]. These cocrystal involve only non-covalent interactions [14–16]. Amongst all oxicams, piroxicam is the safest drug, and many prodrugs like pivoxicam, droxicam, cinnoxicam, and ampiroxicam are available [17,18] Fig. 1 provides the 2D structures of important oxicams.

The *N*-methyl-1,2-thiazine-1,1-dioxide unit of oxicams has been considered an essential structural requirement in oxicams. The enolic-OH group at the 4th position and amide group at the 3rd position as well as the aromatic fused ring at the 5–6 positions of this ring are also the contributing pharmacophoric features of oxicams [19]. The heterocyclic rings carrying mild basicity attached to the amide nitrogen also contribute as a pharmacophoric unit. All the oxicams exhibit extensive tautomerism due to the prototrophic shift originating from the enolic OH group; some of the tautomers are reported in zwitterionic states [4,6].

Toxic side effects have been reported for all oxicams, in a few cases leading to withdrawal or reduced use [20]. For example, tenoxicam may cause gastric irritation, coma, drowsiness, vomiting nausea, headache, tinnitus, and acute renal and kidney failure. Sudoxicam can cause acute liver failure and hepatocellular jaundice, including fatal hepatic necrosis, and was withdrawn from further clinical trials in 1977 [21].

* Corresponding author at: Department of Medicinal Chemistry, National Institute of Pharmaceutical Education and Research (NIPER), Sector-67, S.A.S. Nagar (Mohali), 160062 Punjab, India.
E-mail address: pvbharatam@niper.ac.in (P.V. Bharatam).

https://doi.org/10.1016/j.comptc.2024.114648
Received 21 February 2024; Received in revised form 8 May 2024; Accepted 11 May 2024
Available online 22 May 2024

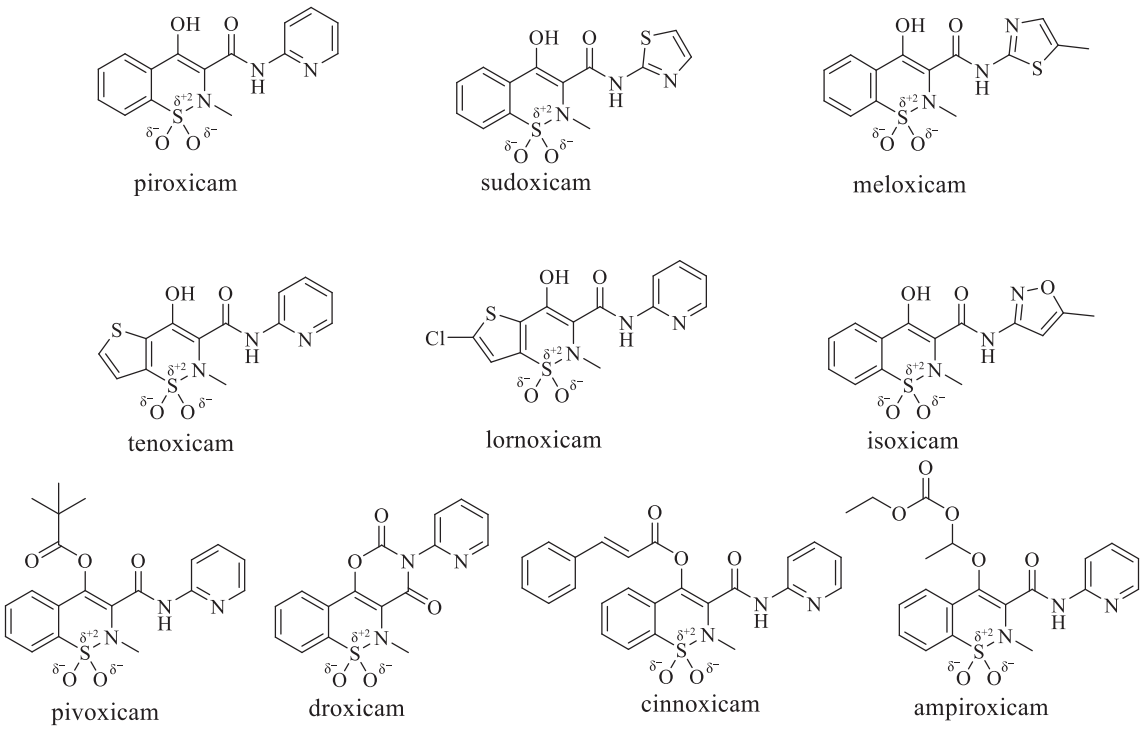

Fig. 1. The 2D structures of important oxicams.

Meloxicam can cause mild gastrointestinal side effects such as dyspepsia, nausea, abdominal pain, and diarrhea [22]. Droxicam causes cholestatic injury [22]. Isoxicam causes toxic epidermal necrolysis associated with hepatic injuries that led to the withdrawal of this drug [21]. Most of these side effects may be attributed to the reactive metabolites originating from these drugs.

The 3D structures of piroxicam [23], lornoxicam [24], droxicam [25], meloxicam [26], and tenoxicam [27], are available in the Cambridge Structural Database (CSD). The 3D structures of oxicams like meloxicam with COX-1 (4O1Z), COX-2 (4M11), and isoxicam with COX-2 (4M10) are available in the Protein Data Bank [28]. Quantum chemical analysis has been carried out on lornoxicam by our group [29]. It was found that the stability of its zwitterionic form is governed by solvent. This study revealed the importance of prototrophic exchange, which governs the existence of polymorphism of this drug in the solid state [29]. Antonov and coworkers [30] performed extensive studies (experimental and theoretical) on the tautomeric transformations of piroxicam in solution. It was found that piroxicam preferred to exist in the sandwich-type dimeric state in ethanol and DMSO. However, in the water medium, the tautomeric equilibrium prefers a zwitterionic state [30]. Glossman-Mitnik and coworkers analyzed the properties of oxicams using conceptual DFT indices [6]. This group also performed theoretical investigations on the spectroscopic properties of oxicams using DFT [31]. Mary *et al.* reported quantum chemical and molecular docking analysis of a few oxicams [32]. A DFT study of the tenoxicam metabolites was carried out by Palomar-Pardavé and coworkers [33].

Only a few reports are available on the metabolic profile of the oxicams, mostly based on mass spectrometry evidence, occasionally using NMR. The 3D structures of possible reactive metabolites of oxicams and their electronic characteristics have not been explored. A conceptual DFT (cDFT) analysis [34–38] of the oxicams has been reported [6] but the corresponding analysis of their metabolites has not been carried out. Quantum chemical analysis can be carried out to calculate the various reactivity descriptors such as global electrophilicity index (ω), and, on that basis, it is possible to identify the reactive metabolite that is most likely responsible for toxic side effects [37,38]. Our group was successful in establishing a possible correlation between the electronic characteristics of metabolites and the observed toxicity profile of a few drugs [39–59]. It was found that many of the metabolites with structural alerts undergo isomerization, and the isomeric forms of the metabolites may often be more crucial towards toxicity. Taking clues from our earlier experience, it is found worthy to explore the electronic structures of oxicams and their metabolites, the results are reported in this article. This comparative study indicated that a few possible metabolites were not considered in earlier studies.

2. Methods

The Gaussian 16 [60] software suite was used to perform DFT calculations of oxicams and their metabolites. The equilibrium geometries of all molecules were determined using gradient techniques to calculate force constants and vibrational frequencies. The hybrid DFT M06 method with the basis set 6–31+G(d,p) was employed in this work [61,62]. M06-class DFT functional was tested in the last decades to be the better compromise between precision to estimate several chemical properties avoiding unpredictable hotspots as seen by hybrid DFT functionals as B3LYP, that M06-class is now considered the standard choice in computational chemistry [63–65]. The absolute energy values chosen for this work include the thermal free energy corrections prescribed in the Gaussian 16 suit of programs.

Several global chemical reactivity descriptors of molecules, such as chemical hardness (η), chemical potential (μ), and electrophilicity index (ω), as well as local reactivity descriptors such as the Fukui function, electrophilicity, and nucleophilicity, have been defined using cDFT [35–38]. The global electrophilicity index (ω), eq. (1) is a promising descriptor for predicting toxicological properties. Parr *et al.* proposed the global electrophilicity index (ω) of a chemical species as the square of electronegativity of a molecule (μ) divided by its chemical hardness (η).

$$\omega = \mu^2/2\eta \tag{1}$$

The electrophilicity index has evolved as one of the crucial conceptual DFT-based descriptors to the study of bio-activities, especially the tox-

Table 1
Ionization potential I, first vertical electron affinity A, global electrophilicity ω, total hardness η, and electronegativity μ of piroxicam, its metabolites and prodrugs estimated using the M06 functional and the 6-31G+(d,p) basis set.[a]

piroxicam	I	A	μ	η	ω
Drug	8.112	1.122	−4.617	6.989	1.525
P-M1	7.969	0.974	−4.471	6.995	1.429
P-M2	8.065	1.209	−4.637	6.856	1.568
P-M3	7.922	0.959	−4.440	6.964	1.416
P-M4	7.843	1.067	−4.455	6.776	1.465
P-M5	8.683	1.039	−4.861	7.644	1.546
P-M6	9.396	0.921	−5.158	8.475	1.570
P-M7	9.741	0.643	−5.192	9.098	1.481
P-M8	10.120	0.722	−5.421	9.397	1.564
P-M9	8.656	2.373	−5.515	6.283	2.420
pivoxicam	7.924	1.113	−4.518	6.811	1.499
droxicam	8.735	1.344	−5.040	7.391	1.718
cinnoxicam	7.948	1.521	−4.734	6.427	1.744
ampiroxicam	8.030	1.117	−4.574	6.912	1.513

[a] All values are expressed in eV units.

icities of chemicals [3]. Popular qualitative chemical concepts such as electronegativity of a molecule (μ), eq. (2) and chemical hardness (*η*), eq. (3) have been provided with rigorous definitions within the purview of cDFT [34–38].

$$\mu = -(I+A)/2 \tag{2}$$

$$\eta = I - A \tag{3}$$

I and A are the ionization potential and electron affinity of the molecules, respectively. The condensed Fukui function is a local density functional descriptor that can be used to calculate the reactivity of each atom in the molecules [62].

3. Results and discussion

Six well-known oxicams and all their experimentally reported metabolites have been considered in this study. In a few cases, theoretically possible metabolite structures were also considered. The electronic structure analysis of the metabolites of each drug is discussed below.

3.1. Piroxicam

Piroxicam is in widespread clinical use as an NSAID. The 3D structures of piroxicam were explored using the quantum chemical method mentioned earlier [6,30,31,66,67]. The tautomeric polymorphism of piroxicam in solid state was reported; it exists in alternative zwitterionic states of the molecule. Various cocrystals of piroxicam have also been explored [68,69]. The most stable tautomer of piroxicam is characterized by an intramolecular hydrogen bond between the oxygen of the carbonyl group and the hydroxyl group. Table 1 lists the electronic characteristics of piroxicam and its important metabolites. Fig. 2 provides the 2D structures of the metabolites of piroxicam.

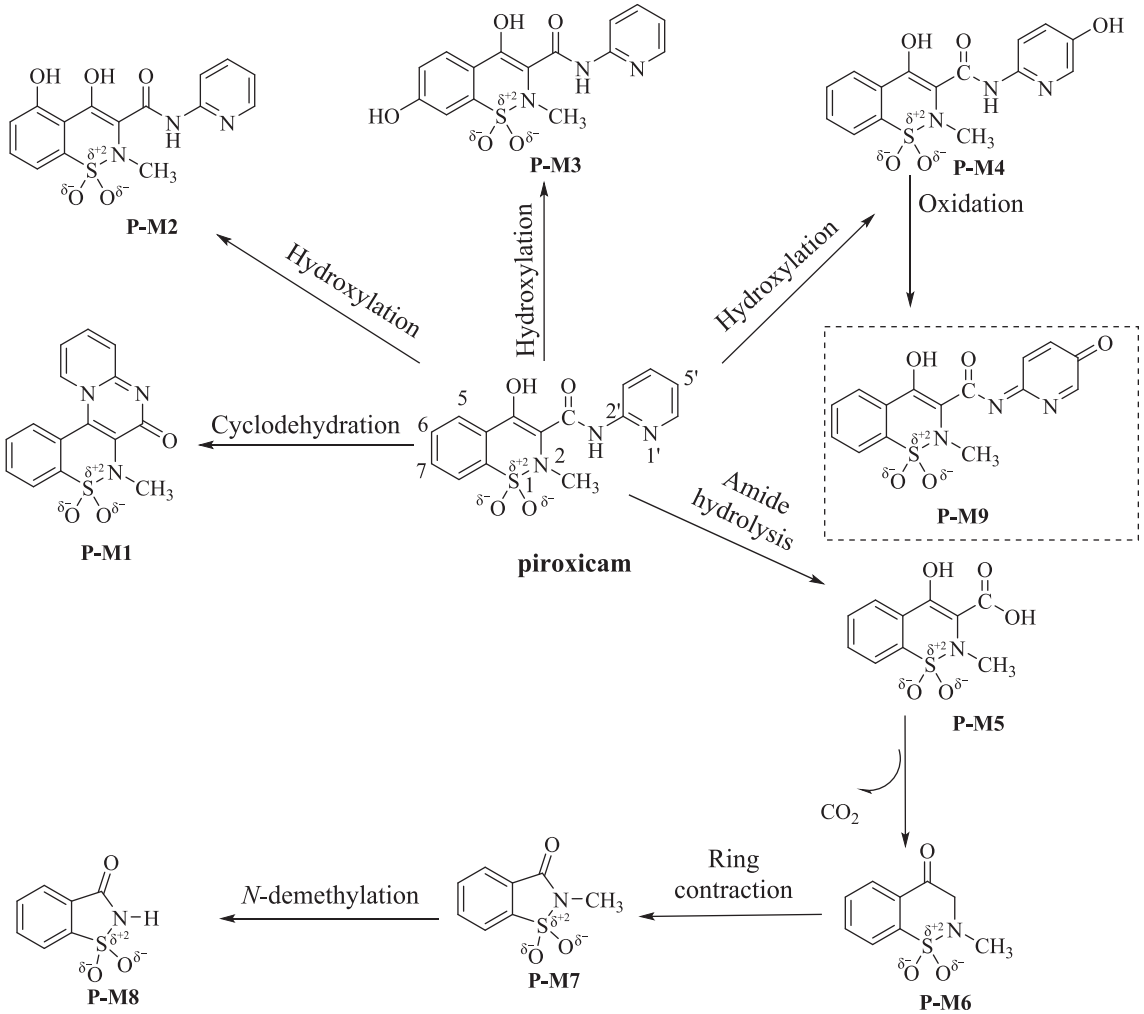

Fig. 2. The metabolic pathway of piroxicam, listing the reported reactive metabolites. The species included in the dashed box is newly considered in this work.

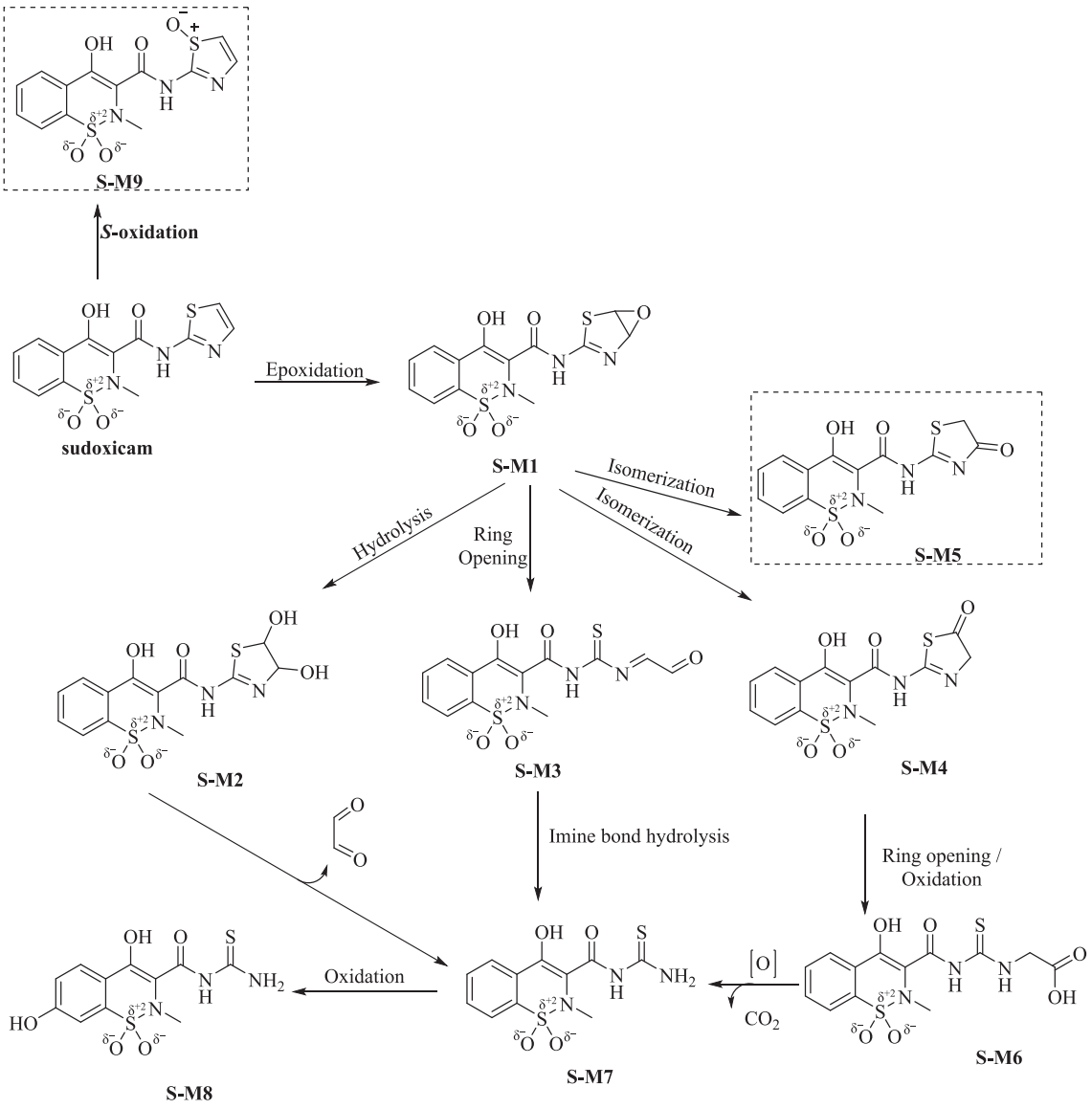

Fig. 3. The metabolic pathway of sudoxicam, listing reported reactive metabolites. The species included in the dashed boxes are newly considered in this work.

Cyclization and dehydration lead to metabolite **P-M1** of piroxicam, which carries a pyrimidinone ring. The cyclodehydration makes **P-M1** safer compared to piroxicam because fewer functional groups are exposed. The metabolites **P-M2** and **P-M3** are products hydroxylated at positions 5 and 7 of the benzothiazine ring system respectively. **PM-4** is hydroxylated at the 5′ position of the pyridine ring. **P-M2** carries two intramolecular hydrogen bonds. **P-M5** is an amide hydrolysis product that is decarboxylated to **P-M6** and further transformed to **P-M7** via ring contraction, followed by *N*-demethylation to **P-M8**. **P-M1** to **P-M8** are all reported to be reactive metabolites, however, none of them was implicated in any toxic side effects. The primary metabolites of piroxicam are the hydroxylated products, their relative energies are in the order **P-M2** (0.00) **<** **P-M3** (2.82) < **P-M4** (5.01 kcal mol^{-1}). All of them were reported experimentally [70]. The global electrophilicity index (ω) value of piroxicam is 1.525 eV and that of all its reported metabolites is < 1.6 eV, thus, all of them are sufficiently safe (ω < 2 eV).

Many drugs are known to form quinonimine metabolites, [71] and this unit is a structural alert because it can act as a Michael acceptor. Following these examples, **P-M4** might get transformed to quinonimine **P-M9** upon oxidation. The electrophilicity index value of **P-M9** is 2.42 eV. This value falls on the borderline toward toxicity (~3 eV) [47]. So far, mild toxicities (gastrotoxicity, photosensitivity) originating from piroxicam have been reported [72]. Considering that the formation of quinonimine might be possible, attention should be paid to the potential toxicity arising from **P-M9**.

To improve the drug delivery of piroxicam, several attempts have been made. This involved prodrug formation as well as the creation of complexes with the polymer. Table 1 also includes the electronic parameters of the prodrugs of piroxicam. All of them have ω values < 1.8 eV. Prodrugs of piroxicam (pivoxicam, droxicam, cinnoxicam, and ampiroxicam) are expected to lead to piroxicam during the first biotransformation and further lead to the metabolites depicted in Fig. 2.

The influence of solvent on the metabolites was evaluated by studying the relative energies of three isomers **P-M2**, **P-M3**, and **P-M4**. Table S2 includes the comparison of the relative energies in the gas phase and the solvent phase. After complete optimization of the structure of these three isomers in implicit water, no significant change has been noticed in the geometries. Similarly, no significant change has been noticed in the relative energy values. Hence, in this work, we continued the analysis of all the oxicams in the gas phase.

Table 2
Ionization potential I, first vertical electron affinity A, global electrophilicity ω, total hardness η, and electronegativity μ of sudoxicam and its metabolites estimated using the M06 functional and the 6-31G+(d,p) basis set[a].

sudoxicam	I	A	μ	η	ω
Drug	8.046	1.258	−4.652	6.788	1.594
S-M1	8.641	1.407	−5.024	7.234	1.744
S-M2	8.587	1.362	−4.975	7.224	1.713
S-M3	8.321	1.886	−5.103	6.435	2.024
S-M4	8.615	1.351	−4.983	7.263	1.709
S-M5	8.807	1.584	−5.196	7.222	1.869
S-M6	8.019	1.254	−4.637	6.764	1.589
S-M7	8.094	1.302	−4.698	6.791	1.625
S-M8	7.929	1.142	−4.538	6.792	1.516
S-M9	8.354	1.688	−5.021	6.666	1.891

[a] All values are expressed in eV units.

3.2. Sudoxicam and meloxicam

Both sudoxicam and meloxicam are oxicams containing a thiazole ring in the side chain, thus they are being studied together and their metabolic profiles are being compared [73]. Sudoxicam is a reversible cyclooxygenase antagonist and a potential NSAID, introduced in 1970 and withdrawn in 1972 due to severe idiosyncratic hepatotoxicity [18]. Meloxicam is a selective inhibitor of cyclooxygenase-2 (COX-2) and an NSAID [22]. Meloxicam is used in the management of rheumatoid arthritis and osteoarthritis, for the short-term symptomatic treatment of acute exacerbations of osteoarthritis, and the symptomatic treatment of ankylosing spondylitis. It may also be used in the treatment of juvenile idiopathic arthritis. Though meloxicam is in use, a few side reactions have been reported.

Obach *et al.* reported the metabolic profile of sudoxicam and meloxicam in human liver microsomes using liquid chromatography–tandem mass spectrometry (LC-MS/MS) and nuclear magnetic resonance (NMR) [73]. Sudoxicam is mostly metabolized via oxidative routes that begin with a thiazole epoxide intermediate (**S-M1**) (Fig. 3). **S-M1** gets hydrolyzed to thiazole-4,5-dihydrodiol (**S-M2**) and ring-opened to an iminoaldehyde (**S-M3**), as well as isomerizes to **S-M4** and **S-M5** after epoxide ring opening. The ring opening of the thiazole ring in **S-M4** leads to the formation of thiohydrotoic acid (**S-M6)** [74]. The decarboxylation of **S-M6** or hydrolysis of **S-M3** give an acylthiourea metabolite (**S-M7**). The hydroxy-acyl thiourea metabolite (**S-M8**) is produced by hydroxylation of the benzothiazine ring of **S-M7** [74–77]. *S*-oxidation is also an important possibility to give **S-M9**. Several sudoxicam metabolites are reactive and contribute to sudoxicam-induced hepatotoxicity [78].

Miller and co-workers carried out a comparative metabolism analysis of meloxicam and sudoxicam using informatics approaches as well as by studying the metabolism using recombinant P450s [79,80]. It was found that CYP2C8 dominates the sudoxicam bioactivation pathway and CYP2C9 dominates the meloxicam detoxification pathway. Our group performed a quantum chemical analysis and established that epoxidation is more favorable in thiazole rings than *S*-oxidation [47]. Also, the various possible isomerization reactions of the preliminary metabolites play a crucial role in determining the toxicity parameters (mainly the electrophilicity (ω) values). However, when the C-5 position in the thiazole ring is blocked with a methyl group, the oxidation at the methyl group becomes more favorable than the epoxidation both in terms of the energy barrier for the metabolic transformation and the stability of the metabolites [73,47]. Thus, the quantum chemical study implied that the preferred oxidation reactions of sudoxicam and meloxicam are distinguishable in terms of kinetics and thermodynamics.

Table 2 lists the electronic parameters estimated using quantum chemical methods on all possible metabolites of sudoxicam given in Fig. 3. The global electrophilicity index value of sudoxicam is 1.594 eV. The metabolites **S-M1**, **S-M3,** **S-M4**, and **S-M5** have global electrophilicity values of 1.744, 2.024, 1.709, and 1.869 eV, respectively. **S-M3** can act as a Michael acceptor and interact with many nucleophiles leading to Mechanism-Based Inhibition (MBI). Particularly, it can interact with glutathione and cause glutathione depletion leading to severe toxicity. **S-M1**, **S-M3**, **S-M4**, **S-M5**, and **S-M9** are all isomers of the epoxide metabolite. The relative energies of these isomers are in the order of **S-M5** (−27.09) < **S-M4** (–23.34) < **S-M1** (0.00) < **S-M3** (6.18) < **S-M9** (32.33 kcal mol^{-1}). These relative values indicate that **S-M9** formation is thermodynamically unlikely, but the conversion of **S-M1** to other isomers is feasible. The functional units in **S-M1** and **S-M3** are structural alerts, thus, it is worth considering the local electrophilicity of these species. Quantum chemical studies showed that iminoaldehydes are highly electrophilic and, thus, can lead to MBI [47]. The metabolite **S-M5** was not considered in earlier studies but is the most stable isomer on the energy scale. As it is an energetically preferred isomer, attempts should be made to identify it experimentally.

In vitro studies indicated that CYP2C9 plays an important role in the metabolic pathway of meloxicam with a minor contribution of the CYP3A4 isozyme [22]. Meloxicam only differs from sudoxicam by a methyl group at the C-5 position of the thiazole ring, and due to the hydroxylation of this methyl group, meloxicam undergoes a competitive detoxification pathway [74]. Furthermore, the probability of epoxidation in meloxicam has been reported to be lower because of the C-5 substitution in the thiazole ring.

Sashidhar *et al.* reported the meloxicam metabolism of the *Cunninghamella blakesleeana* fungus species [81]. It results in the two major metabolites 5-hydroxy methyl meloxicam (**M−M1**) and 5-carboxy methyl meloxicam (**M−M2**), which are formed by the oxidation of the methyl group at the C-5 position of the thiazole ring. The metabolites were identified by HPLC and LC-MS spectrometry [81]. In humans, the enzyme CYP3A4 is also responsible for the formation of **M−M1** as reported by Chesne and coworkers [82]. Davies and Skjodt *et al.* also reported **M−M1** and **M−M2** metabolites of meloxicam and claimed that these metabolites are pharmacologically inactive and excreted from the body via urine and faeces [83].

Obach *et al.* provided a detailed scheme for the metabolism of meloxicam [73]. (Fig. 4). Miller *et al.* reported the formation of the epoxide metabolite (**M−M4**) via epoxidation followed by hydrolysis, which gave 5-methyl-4,5-dihydrothiazole-4,5-diol (**M−M5**). The ring scission of **M−M4** yields iminoaldehyde **M−M7** and is followed by hydrolysis to form the acyl thiourea **M−M9** [79,80]. The metabolite **M−M9** gets converted into the hydroxy-acyl thiourea **M−M12** and **M−M10**, which is formed by cyclization [73]. The metabolite **M−M8** may be formed through the reduction of the imine intermediate of the opening of the thiazole ring (**M−M7**), but this metabolite is only observed in the presence of GSH. The metabolites **M−M7**, **M−M9**, and **M−M12** are similar to the metabolites of sudoxicam **S-M3**, **S-M6**, and **S-M7,** respectively. **M−M13** is the *S*-oxidation metabolite of meloxicam.

A quantum chemical study has been performed to find out the global electrophilicity of meloxicam and its metabolites to assess potential toxicity (Table 3). **M−M1**, **M−M4**, **M−M7**, **M−M11**, and **M−M13** are isomers. Their relative stabilities are in the order of **M−M14** (−17.07) < **M−M1** (0.00) < **M−M7** (11.88) < **M−M4** (12.62) < **M−M11** (15.50) < **M−M13** (45.49 kcal mol^{-1}). On a thermodynamic basis, it can be concluded that the formation of the *S*-oxidation metabolite **M−M13** is not likely; experimentally, this isomer has not been reported. Likewise, it can be inferred that the keto isomer **M−M14** formed from the isomerization of the epoxide metabolite is energetically the most favorable metabolite, although it has not been reported from experiments either. The newly identified **M−M14** should be considered in future studies on the metabolism of meloxicam.

Table 3 indicates that the metabolites of meloxicam are generally safe (electrophilicity index < 2 eV). However, **M−M7** is more electrophilic compared to the others and because of the iminoaldehyde character, it may behave as a Michael acceptor. Epoxide metabolites are prone to acid-catalyzed ring-opening to produce enols and subsequently

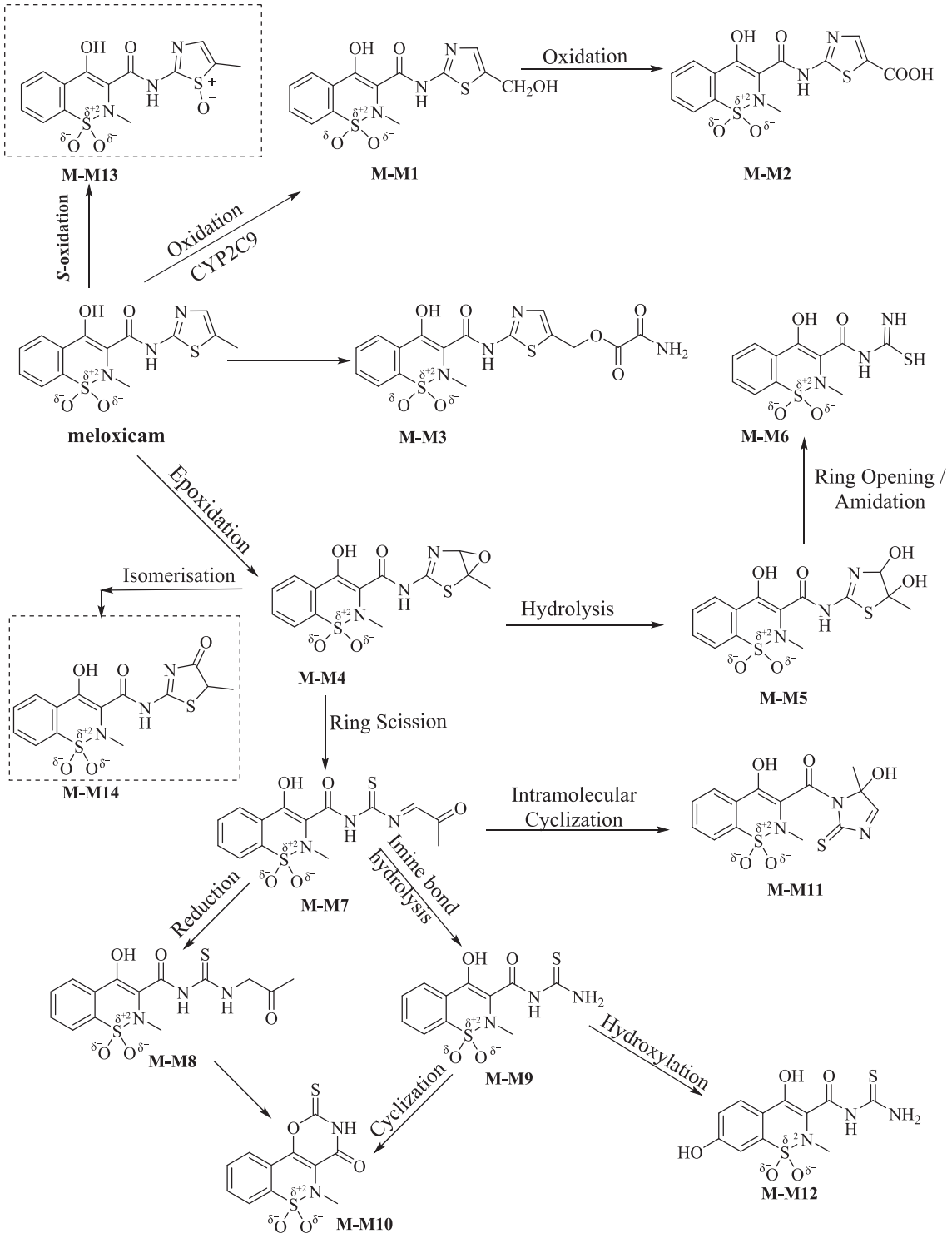

Fig. 4. The metabolic pathway of meloxicam, listing the reported reactive metabolites. The species included in the dashed boxes are newly considered in this work. Figure adapted from ref [73].

tautomerize to produce double keto derivatives [84]. As a result, under acidic conditions, sudoxicam, as well as meloxicam, can in principle undergo tautomerization to the keto derivatives (Fig. 5). However, there are a few interesting differences. In the case of sudoxicam, epoxidation is the most favorable metabolic reaction, the formation of **S-M1** is highly preferred, and subsequent isomerizations to **S-M4** and **S-M5** are also favorable. In the case of meloxicam, epoxidation is less favorable and, thus, the probability of finding **M**−**M4** is very small, consequently the probability of finding **M**−**M14** during metabolic reactions is also very small.

3.3. *Tenoxicam*

Tenoxicam received medical approval in 1987 in a few countries. The reported side effects of tenoxicam are peptic ulceration, dyspepsia, nausea, constipation, abdominal pain, diarrhea, rash, headache, edema, renal failure, vertigo, Stevens-Johnson syndrome, and toxic epidermal necrolysis [85]. The metabolites of tenoxicam get eliminated mainly by

Table 3
Ionization potential I, first vertical electron affinity A, global electrophilicity ω, total hardness η, and electronegativity μ of meloxicam and its metabolites estimated using the M06 functional and the 6-31G+(d,p) basis set.[a.]

meloxicam	I	A	μ	η	ω
Drug	7.816	1.217	−4.517	6.598	1.546
M−M1	7.810	1.229	−4.519	6.581	1.552
M−M2	8.296	1.531	−4.913	6.765	1.784
M−M3	8.047	1.359	−4.703	6.688	1.654
M−M4	8.558	1.363	−4.960	7.194	1.710
M−M5	8.490	1.323	−4.907	7.168	1.679
M−M6	8.094	1.302	−4.698	6.791	1.625
M−M7	8.291	1.975	−5.133	6.315	2.086
M−M8	7.938	1.218	−4.578	6.719	1.560
M−M9	8.094	1.302	−4.698	6.791	1.625
M−M10	8.416	1.458	−4.937	6.958	1.752
M−M11	8.131	1.722	−4.927	6.409	1.893
M−M12	7.934	1.142	−4.538	6.792	1.516
M−M13	8.171	1.603	−4.887	6.568	1.818
M−M14	8.742	1.654	−5.198	7.088	1.906

[a] All values are in eV units.

the renal route as 5'-hydroxy tenoxicam, whereas excretion via the bile is in the form of the C-6 glucuronide of tenoxicam [86]. Ring contraction and ring chain tautomerism are reported for this drug under in vivo conditions. Electronic structure analysis and spectro-electrochemical studies were reported for tenoxicam and its toxic metabolites [33].

Ichihara *et al.* reported the metabolism of tenoxicam via a hydroxylation and oxidation pathway [87] (Fig. 6). Palomar-Pardavé *et al.* also reported the formation of several metabolites using electrochemical oxidation of tenoxicam [33]. According to the literature, **T-M1** is formed due to hydroxylation at the C-5 position of the pyridine ring [87], which may be converted into the quinonimine metabolite **T-M4** that has not been reported. The hydroxylation of tenoxicam at the C-6 position of the thiophene ring (presumably after initial epoxidation to **T-M2**) leads to the formation of **T-M5** and **T-M6,** and further isomerization may result in the formation of **T-M7** and **T-M8,** respectively (Fig. 6). Many smaller metabolites are reported for this drug (Figure S1, ESI) [87].

Our group reported the possible oxidation pathways of the thiophene ring [53]. It was found that epoxidation is more favorable than *S*-oxidation by ~ 16.70 kcal mol^{-1}. Furthermore, it was found that the isomerization of the epoxide can lead to hydroxy and keto isomers, which are more stable (by ~ 25 kcal mol^{-1}). In this work, a few possible metabolites of tenoxicam that have not been reported from experimental studies were also considered. The relative stability of isomeric metabolites of tenoxicam is in the order **T-M7** (−2.07) < **T-M1** (0.00) < **T-M6** (1.72) < **T-M5** (2.21) < **T-M8** (2.58) < **T-M2** (29.5) < **T-M3** (55.03 kcal mol^{-1}).

This work implies that the relative stability based on energy also plays an important role in metabolism. The relative energy implies that

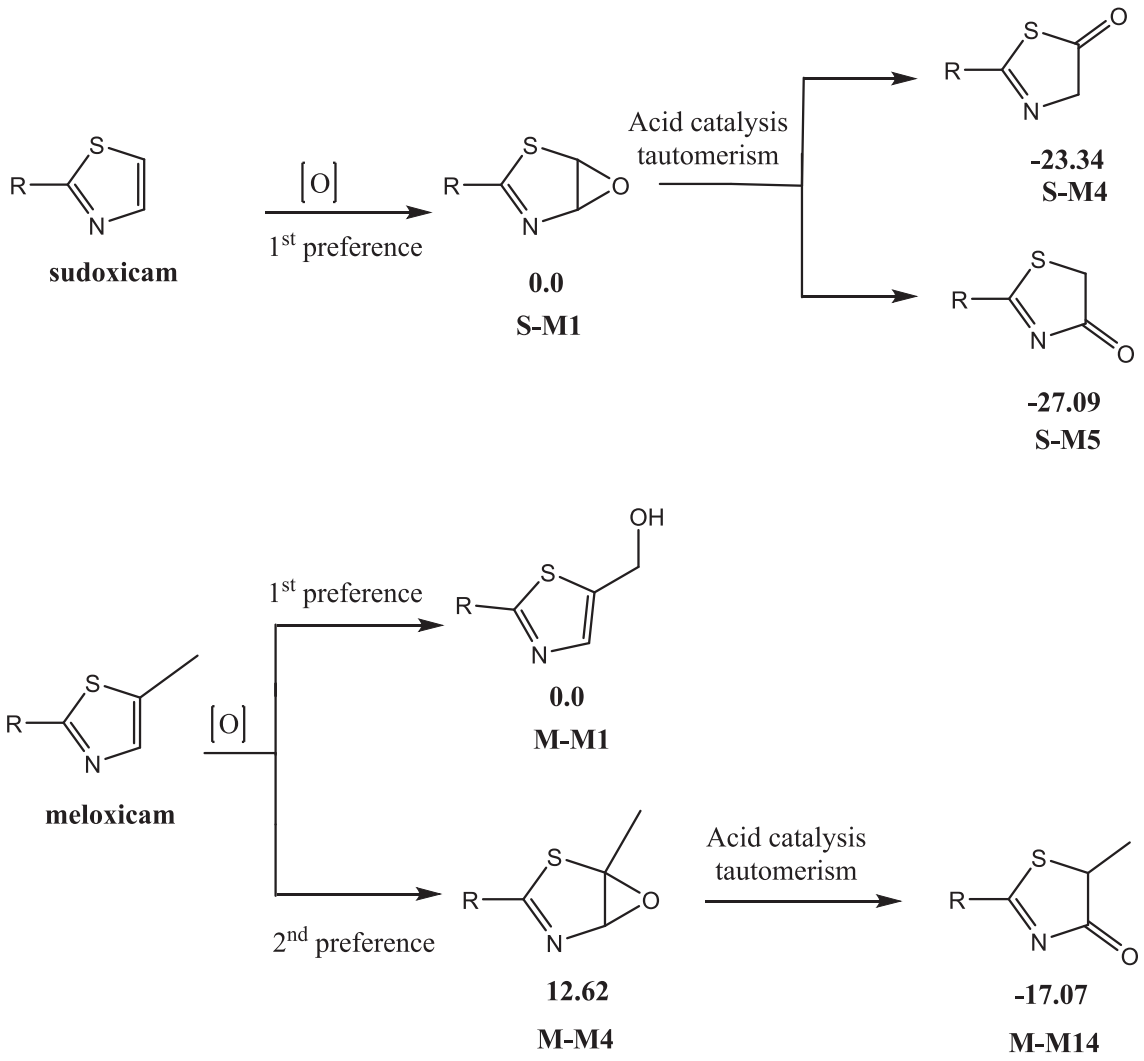

Fig. 5. Comparative energy analysis of epoxide formation and the corresponding keto isomers of sudoxicam and meloxicam. The relative energy values on the respective potential energy surfaces are in kcal/mol.

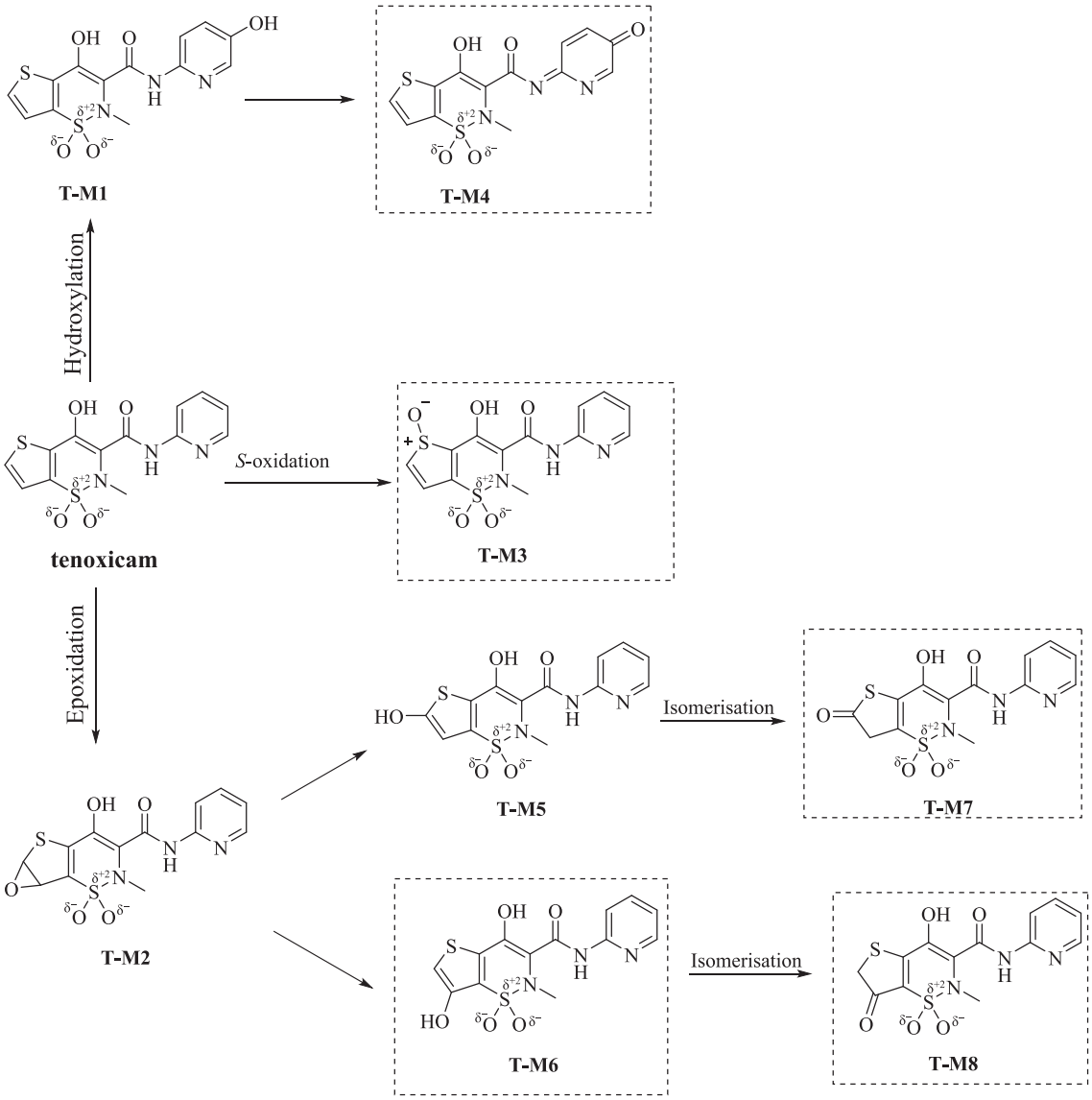

Fig. 6. The metabolic pathway of tenoxicam, listing the reported reactive metabolites. The species included in the dashed boxes are newly considered in this work.

Table 4
Ionization potential I, first vertical electron affinity A, global electrophilicity ω, total hardness η, and electronegativity μ of tenoxicam and its metabolites estimated by using the M06 functional and the 6-31G+(d,p) basis set.[a].

tenoxicam	I	A	μ	η	ω
Drug	8.076	1.264	−4.670	6.812	1.601
T-M1	7.803	1.206	−4.505	6.597	1.538
T-M2	8.311	1.574	−4.942	6.736	1.813
T-M3	8.278	2.113	−5.196	6.165	2.189
T-M4	8.596	2.419	−5.508	6.177	2.456
T-M5	7.841	1.130	−4.485	6.712	1.499
T-M6	8.036	1.375	−4.706	6.660	1.662
T-M7	8.372	1.568	−4.970	6.803	1.815
T-M8	8.471	2.012	−5.241	6.459	2.127

[a] All values are in eV units.

the *S*-oxide **T-M3** and epoxide **T-M2** are not energetically favorable. Indeed, experimental metabolism studies did not report these species. This is encouraging because these two positions would be considered prone to metabolism on the basis of the structural alert thiophene [53]. However, all other species in this series are accessible according to the relative energy scale, especially **T-M6** and **T-M7**, which were not considered in earlier studies. The other two isomers **T-M5** and **T-M8** are also important according to the relative energy scale.

From the cDFT study, it was found that the drug and most of its metabolites are safe because the global electrophilicity index values are < 2 eV, but **T-M4** exhibits a global electrophilicity index value of 2.456 eV (Table 4). This metabolite has not been reported by earlier studies. The quinonimines are known to be structural alerts and, thus, the importance of **T-M4** in the observed toxicity of tenoxicam needs to be explored [33,87].

3.4. Lornoxicam

Lornoxicam (chlortenoxicam) is an NSAID known to reduce prostaglandin synthesis. It is highly potent and structurally different from tenoxicam only by a chloro substitution at the C-6 position of the thiophene ring. This drug differs from the other oxicams in terms of its short half-life and rapid elimination. The drug is excreted as a metabolite, and no unchanged drug is found in urine [19]. It has been available in Switzerland and some other European countries since 1995 [88]. Zhang *et al.* reported the polymorphic form of lornoxicam followed by its characterization through FTIR, DSC, XRD, and thermogravimetric method [89], and its pK_a was studied by Ho *et al.* [90]. The tautomeric

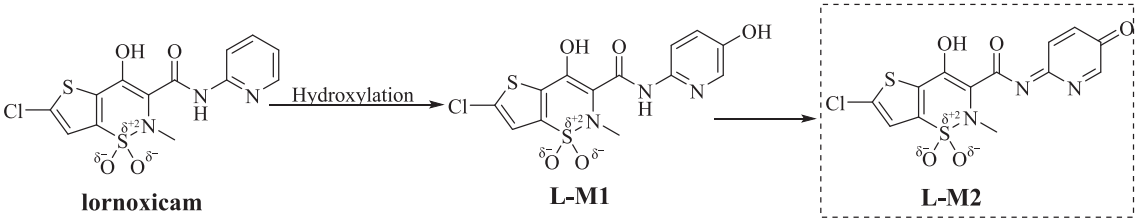

Fig. 7. The CYP450-mediated metabolism of lornoxicam. The species included in the dashed box are newly considered in this work.

Table 5
Ionization potential I, first vertical electron affinity A, global electrophilicity ω, total hardness η, and electronegativity μ of lornoxicam and its metabolites estimated using the M06 functional and the 6-31G+(d,p) basis set.[a].

lornoxicam	I	A	μ	η	ω
Drug	8.080	1.452	−4.766	6.628	1.713
L-M1	2.929	−2.929	0.000	5.859	0.000
L-M2	8.561	2.505	−5.533	6.056	2.527

[a] All values are in eV units.

vs. zwitterionic preferences of lornoxicam and its correlation to the solid state properties were reported by Nathavad *et al.* [29].

Only one reactive metabolite of lornoxicam (**L-M1**) has been reported [91]. After CYP-mediated oxidation (Fig. 7), the glucuronide conjugates are excreted through urine and feces. The global electrophilicity index values of lornoxicam and **L-M1** are < 1.6 eV, hence, the drug and metabolite are relatively safe (Table 5). The formation of **L-M1** is determined by the three major human drug-metabolizing CYP450 isozymes CYP2C9, CYP2D6, and CYP3A4 in healthy, young, and elder volunteers (Table 5) [6,92,93]. The single reported metabolite of lornoxicam can be attributed to the presence of the chloro substituent on

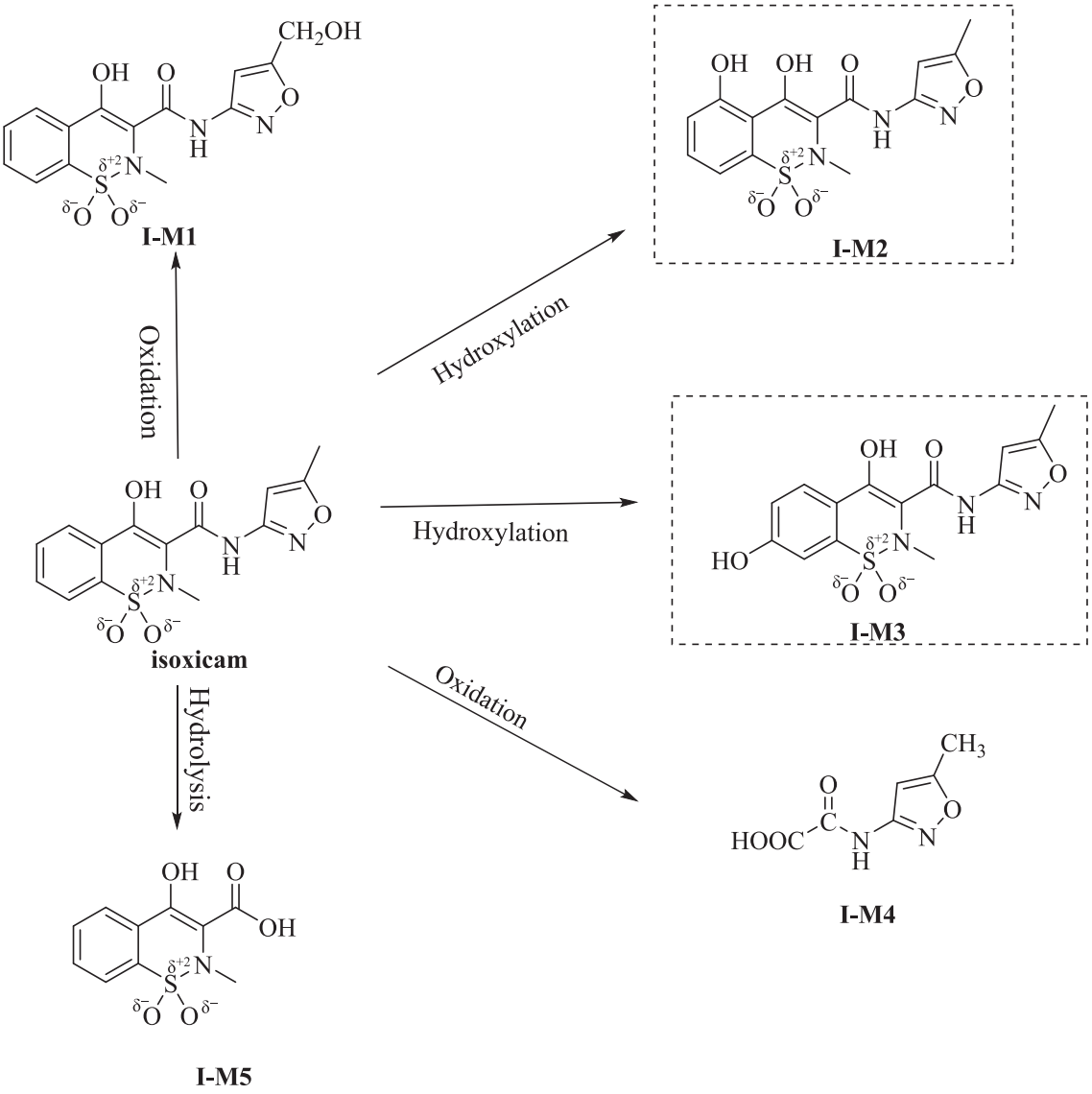

Fig. 8. The metabolic pathway of isoxicam, listing the reported reactive metabolites. The species included in the perforated box is newly considered in this work.

Table 6
Ionization potential I, first vertical electron affinity A, global electrophilicity ω, total hardness η, and electronegativity μ of isoxicam and its metabolites estimated using the M06 functional and the 6-31G+(d,p) basis set.[a].

isoxicam	I	A	μ	η	ω
Drug	8.382	1.153	−4.768	7.229	1.572
I-M1	8.417	1.181	−4.799	7.236	1.592
I-M2	8.294	1.240	−4.767	7.054	1.611
I-M3	8.158	0.981	−4.569	7.176	1.455
I-M4	9.294	0.332	−4.813	8.962	1.292
I-M5	8.683	1.039	−4.861	7.643	1.546

[a] All values are in eV units.

Table 7
Enzymes responsible for metabolism of the drugs, reported toxic metabolites and predicted metabolites from our study.

Drug	Major Metabolising enzymes	Possible newly predicted metabolites
piroxicam	CYP2C9	P-M9
sudoxicam	CYP2C8	S-M5, S-M9
meloxicam	CYP2C9, CYP3A4	M−M13, M−M14
tenoxicam	CYP2C9	T-M3, T-M4, TM-6, TM-7, T-M8
lornoxicam	CYP2C9, CYP2D6, CYP3A4	L-M2
isoxicam	CYP3A	I-M3, I-M2

the thiophene ring. The substituent precludes epoxide formation and subsequent isomerization, thus reducing the number of possible metabolites. However, considering the structural similarity with tenoxicam, the quinonimine metabolite **L-M2** might need to be considered. The DFT study established that **L-M2** has a high electrophilicity index value of 2.527 eV, which suggests a possible toxicity emerging from **L-M2**. Experimental studies are required to confirm this hypothesis.

3.5. Isoxicam

Isoxicam was used for the treatment of rheumatoid arthritis disorders until its marketing was suspended worldwide because of fatal skin reactions. In 1985, isoxicam was withdrawn from the French market due to adverse effects, namely toxic epidermal necrolysis, also called Lyell syndrome, resulting in death [94].

Woolf *et al.* reported the CYP450-mediated oxidative metabolism of isoxicam in rats, dogs, monkeys, and humans [95]. Isoxicam forms a hydroxymethyl metabolite (**I-M1**) due to the methyl group of the isoxazole ring (Fig. 8). In comparison to the metabolites reported for piroxicam, **I-M2** and **I-M3** are also possible but have not been reported earlier. The hydrolysis of the amide bond has been reported to produce **I-M4** and **I-M5**; the latter is the same as **P-M5** of piroxicam. The decarboxylation, ring contraction, and *N*-demethylation reactions reported for **P-M5** were observed in the case of **I-M5** as well [95,96].

Quantum chemical analysis of isoxicam and its metabolites has been performed to analyze the relative energy and toxicity of the drug and its reactive metabolites (Table 6). The relative energies of the primary metabolites of isoxicam are **I-M2** (−14.91) < **I-M3** (−12.25) < **I-M1** (0.00 kcal mol^{-1}). Experimentally, **I-M2** and **I-M3** were not reported [95,96], however, similar hydroxylation products were reported for piroxicam. This comparative analysis indicates that it is worth exploring the possibility of the relatively more stable metabolites **I-M2** and **I-M3** in future studies. According to cDFT analysis, it can be concluded that the drug and all of its metabolites are safe due to low global electrophilicity values (<2 eV) (Table 6). The observed skin reactions may thus not be related to the electronic characteristics of the drug or its metabolites.

Table 7 includes a summary of the results from this work. The metabolites which are newly predicted in this study are listed in the table. This work highlights the importance of including the DFT calculations of the possible metabolites along with the mass spectral analysis of metabolites formation during the metabolism of the drugs.

4. Conclusions

Quantum chemical analysis using DFT has been carried out to study the electronic structure of the metabolites of drugs of the oxicam class. The M06/6–31+G(d,p) level of quantum chemical calculations provided many important details, particularly concerning metabolites **P-M9**, **S-M5**, **T-M4**, and **L-M2**. Such information is complementary to the results obtained from mass spectrometry and other physicochemical studies on the metabolism of drugs. In this comparative analysis, new possible metabolites have been suggested in addition to the experimentally reported ones. The major conclusion emerging from this analysis is that it is essential to consider many isomeric states of the metabolites and their relative energies, in addition to experimental characterization. Based on this observation, it can be suggested that future studies on drug metabolism should incorporate the electronic structure analysis of all possible isomers of the drug metabolites. Some isomers may be eliminated based on relative energies, and additional efforts can then be focussed on characterizing the energetically more stable isomers of metabolites. Using cDFT theory, the characteristic features of the reactive metabolites can be evaluated and compared. The metabolites with large electrophilicity index values (ω) may be prioritized further for toxicity studies.

5. Data and Software Availability

The quantum chemical information with the archive data for the oxicams and their metabolites are provided in the supporting information file at https://drive.google.com/drive/folders/1imuodAF2AJBzClDvryFUe7ClqjdDDBNs?usp=drive_link.

CRediT authorship contribution statement

Joydeep Burman: Formal analysis, Data curation, Conceptualization. **Kanika Manchanda:** Writing – review & editing. **Kaushikkumar A. Bhakhar:** Writing – original draft. **Akshay N. Boharupi:** Data curation. **Holger Gohlke:** Writing – review & editing. **Prasad V. Bharatam:** Writing – review & editing, Validation, Resources, Methodology, Investigation, Funding acquisition, Formal analysis, Data curation, Conceptualization.

Declaration of competing interest

The authors declare that they have no known competing financial interests or personal relationships that could have appeared to influence the work reported in this paper.

Data availability

The google drive link has been provided in data availability section

Acknowledgments

The authors thank the Department of Biotechnology (DBT), Govt. of India (GOI), New Delhi (grant number: BT/IN/BMBF-BioHR/30/PVB/2018-2019) and the Bundesministerium für Bildung und Forschung, Germany (BMBF) (funding number: 01DQ19002) for financial support within the project ReMetaDrug.

References

[1] N. Ishihama, S.W. Choi, Y. Noutoshi, I. Saska, S. Asai, K. Takizawa, S.Y. He, H. Osada, K. Shirasu, Oxicam-type non-steroidal anti-inflammatory drugs inhibit NPR1-mediated salicylic acid pathway, Nat. Commun. 12 (2021) 7303–7315, https://doi.org/10.1038/s41467-021-27489-w.

[2] C.A. Rouzer, L.J. Marnett, Structural and chemical biology of the interaction of cyclooxygenase with substrates and non-steroidal anti-inflammatory drugs, Chem. Rev. 120 (2020) 7592–7641, https://doi.org/10.1021/acs.chemrev.0c00215.

[3] Y. Shamsudin, H. Gutiérrez-de-Terán, J. Åqvist, Molecular mechanisms in the selectivity of nonsteroidal anti-inflammatory drugs, Biochemistry. 57 (2018) 1236–1248, https://doi.org/10.1021/acs.biochem.7b01019.

[4] P.V. Bharatam, O.R. Valanju, A.A. Wani, D.K. Dhaked, Importance of tautomerism in drugs, Drug Discov. Today 4 (2023) 103494, https://doi.org/10.1016/j.drudis.2023.103494.

[5] S.G. Arkhipov, P.S. Sherin, A.S. Kiryutin, V.A. Lazarenko, C. Tantardini, The role of S-bond in tenoxicam keto–enolic tautomerization, CrystEngComm. 21 (2019) 5392–5401, https://doi.org/10.1039/C9CE00874H.

[6] J.I. Martínez-Araya, G. Salgado-Morán, D. Glossman-Mitnik, Computational nanochemistry report on the oxicams-conceptual DFT indices and chemical reactivity, J. Phys. Chem. b. 117 (2013) 6339–6351, https://doi.org/10.1021/jp400241q.

[7] S. Nita, A.A. Andries, L. Patron, R. Albulescu, F. Radulescu, C. Tanase, Analytical and toxicological characterization of new Co(II) coordination compounds with antiinflammatory oxicams drugs, Rev. Chim. 62 (2011) 549–553.

[8] C. Tantardini, E.V. Boldyreva, E. Benassi, Hypervalency in organic crystals: a case study of the oxicam sulfonamide group, J. Phys. Chem. a. 120 (2016) 10289–10296, https://doi.org/10.1021/acs.jpca.6b10703.

[9] R.S. Tsai, P.A. Carrupt, N. Tayar, El, Y. Giroud, P. Andrade, B. Testa, F. Brée, J. P. Tillement, Physicochemical and structural properties of non-steroidal anti-inflammatory oxicams, Helv. Chim. Acta. 76 (1993) 842–854, https://doi.org/10.1002/hlca.19930760208.

[10] C. Tantardini, S.G. Arkhipov, K.A. Cherkashina, A.S. Kil'met'ev, E.V. Boldyreva, Crystal structure of a 2:1 co-crystal of meloxicam with acetylendicarboxylic acid, Acta Cryst. Sec. e: Cryst. Comm. 72 (2016) 1856–1859, https://doi.org/10.1107/S2056989016018909.

[11] A.G. Ogienko, S.A. Myz, A.A. Ogienko, A.A. Nefedov, A.S. Stoporev, M. S. Mel'gunov, A.S. Yunoshev, T.P. Shakhtshneider, V.V. Boldyrev, E.V. Boldyreva, Cryosynthesis of co-crystals of poorly water-soluble pharmaceutical compounds and their solid dispersions with polymers. the "Meloxicam–Succinic Acid" System as a case study, Cryst. Growth Des. 18 (2018) 7401–7409, https://doi.org/10.1021/acs.cgd.8b01070.

[12] C. Tantardini, S.G. Arkhipov, K.A. Cherkashina, E.V. Boldyreva, Synthesis and crystal structure of a meloxicam co-crystal with benzoic acid, Struct. Chem. 29 (2018) 1867–1874, https://doi.org/10.1007/s11224-018-1166-5.

[13] K. Fucke, S.A. Myz, T.P. Shakhtshneider, E.V. Boldyreva, U.J. Griesser, How good are the crystallisation methods for co-crystals? A comparative study of piroxicam, New J. Chem. 36 (2012) 1969–1977, https://doi.org/10.1039/C5RA03653D.

[14] G. Resnati, E. Boldyreva, P. Bombicz, M. Kawano, Supramolecular interactions in the solid state, IUCrJ 2 (2015) 675–690, https://doi.org/10.1107/S2052252515014608.

[15] N.A. Tumanov, S.A. Myz, T.P. Shakhtshneider, E.V. Boldyreva, Are meloxicam dimers really the structure-forming units in the'meloxicam−carboxylic acid'cocrystals family? Relation between crystal structures and dissolution behaviour, CrystEngComm 14 (2012) 305–315, https://doi.org/10.1039/C1CE05902E.

[16] A.Y. Fedorov, T.N. Drebushchak, C. Tantardini, Seeking the best model for noncovalent interactions within the crystal structure of meloxicam, Comput. Theor. Chem. 1157 (2019) 47–53, https://doi.org/10.1016/j.comptc.2019.04.012.

[17] M. Mihalić, H. Hofman, J. Kuftinec, B. Krile, V. Čaplar, F. Kajfež, N. Blažević, Piroxicam, analytical profiles of drug substances, Academic Press: New York. 15 (1986) 509–531, https://doi.org/10.1016/S0099-5428(08)60422-0.

[18] K.T. Olkkola, A.V. Brunetto, M.J. Mattila, Pharmacokinetics of oxicam nonsteroidal anti-inflammatory agents, Clin. Pharmacokinet. 26 (1994) 107–120, https://doi.org/10.2165/00003088-199426020-00004.

[19] N.M. Skjodt, N.M. Davies, Clinical pharmacokinetics of lornoxicam: a short half-life oxicam, Clin. Pharmacokinet. 34 (1998) 421–428, https://doi.org/10.2165/00003088-199834060-00001.

[20] T. Harr, L.E. French, Toxic epidermal necrolysis and Stevens-Johnson syndrome, Orphanet J. Rare Dis. 5 (2010) 1–11, https://doi.org/10.1016/j.mcna.2010.04.004.

[21] H. Dancygier, Hepatic Biotransformation, Clinical Hepatology; Springer: Berlin, Heidelberg 1 (2010) 127–130, https://doi.org/10.1007/978-3-540-93842-2_8.

[22] S. Noble, J.A. Balfour, Meloxicam, Drugs. 51 (1996) 424–430, https://doi.org/10.2165/00003495-199651030-00007.

[23] S. Modani, A. Gunnam, B. Yadav, A.K. Nangia, N.R. Shastri, Generation and evaluation of pharmacologically relevant drug-drug cocrystal for gout therapy, Cryst. Growth Des. 20 (2020) 3577–3583, https://doi.org/10.1021/acs.cgd.0c00106.

[24] K. Suresh, A. Nangia, Lornoxicam salts: crystal structures, conformations, and solubility, Cryst. Growth Des. 14 (2014) 2945–2953, https://doi.org/10.1021/cg500231z.

[25] J. Frigola, Study of the structure of Droxicam, 5-methyl-3-(2-pyridyl)-2H,5H–1,3-oxazino [5,6-c][1,2]benzothiazine-2, 4(3 H)-dione 6,6-dioxide, using X-ray crystallography and 1H and 13C nuclear magnetic resonance spectroscopy, J. Chem. Soc., Perkin Trans. 2 (1988) 241–245, https://doi.org/10.1039/P29880000241.

[26] G.F. Fabiola, V. Pattabhi, S.G. Manjunatha, G.V. Rao, K. Nagarajan, 4-Hydroxy-2-methyl-N-(5-methyl-1, 3-thiazol-2-yl)-2H-1,2-benzothiazine-3-carboxamide 1, 1-dioxide, Acta Crystallogr. C Struct. Chem 54 (1998) 2001–2003, https://doi.org/10.1107/S0108270198008452.

[27] G. Bolla, P. Sanphui, A. Nangia, Solubility advantage of tenoxicam phenolic cocrystals compared to salts, Cryst. Growth Des. 13 (2013) 1988–2003, https://doi.org/10.1021/cg4000457.

[28] S. Xu, D.J. Hermanson, S. Banerjee, K. Ghebreselasie, G.M. Clayton, R.M. Garavito, L.J. Marnett, Lipids: oxicams bind in a novel mode to the cyclooxygenase active site via a two-water-mediated h-bonding network, J. Biol. Chem. 289 (2014) 6799–6808, https://doi.org/10.1074/jbc.M113.517987.

[29] Z.P. Nathavad, S. Bhatia, D.K. Dhaked, P.V. Bharatam, Electronic structure analysis of isomeric preferences of canonical and zwitterionic forms of lornoxicam, Comput. Theor. Chem. 1023 (2013) 51–58, https://doi.org/10.1016/j.comptc.2013.09.011.

[30] D. Ivanova, V. Deneva, D. Nedeltcheva, F.S. Kamounah, G. Gergov, P.E. Hansen, S. Kawauchi, L. Antonov, Tautomeric transformations of piroxicam in solution: a combined experimental and theoretical study, RSC Adv. 5 (2015) 31852–31860, https://doi.org/10.1039/C5RA03653D.

[31] A.G. Pacheco, G. Salgado-Morán, L. Gerli-Candia, R. Ramírez-Tagle, D. Glossman-Mitnik, A. Misra, A.F. de Carvalho Alcantara, Theoretical investigation of the molecular structure and spectroscopic properties of oxicams, J. Struct. Chem. 58 (2017) 261–267, https://doi.org/10.1134/S0022476617020068.

[32] Y.S. Mary, Y.S. Mary, K.S. Resmi, R. Thomas. DFT and molecular docking investigations of oxicam derivatives, Heliyon. 5 (2019) e02175–e02182. Doi: 10.1016/j.heliyon.2019.e02175.

[33] M.T. Ramírez-Silva, D.S. Guzmán-Hernández, A. Galano, A. Rojas-Hernández, S. Corona-Avendaño, M. Romero-Romo, M. Palomar-Pardave, Spectro-electrochemical and DFT study of tenoxicam metabolites formed by electrochemical oxidation, Electrochim. Acta. 111 (2013) 314–323, https://doi.org/10.1016/j.electacta.2013.07.191.

[34] R.G. Parr, L.V. Szentpály, S. Liu, Electrophilicity index, J. Am. Chem. Soc. 121 (1999) 1922–1924, https://doi.org/10.1021/ja983494x.

[35] P.K. Chattaraj, D.R. Roy, Update 1 of: electrophilicity index, Chem. Rev. 107 (2007) 46–74, https://doi.org/10.1021/cr078014b.

[36] P.K. Chattaraj, S. Duley, Electron affinity, electronegativity, and electrophilicity of atoms and ions, J. Chem. Eng. Data. 55 (2010) 1882–1886, https://doi.org/10.1021/je900892p.

[37] D.R. Roy, U. Sarkar, P.K. Chattaraj, A. Mitra, J. Padmanabhan, R. Parthasarathi, V. Subramanian, S. Van Damme, P. Bultinck, Analyzing toxicity through electrophilicity, Mol. Divers. 10 (2006) 119–131, https://doi.org/10.1007/s11030-005-9009-x.

[38] D.R. Roy, R. Parthasarathi, B. Maiti, V. Subramanian, P.K. Chattaraj, Electrophilicity as a possible descriptor for toxicity prediction, Bioorg. Med. Chem. 13 (2005) 3405–3412, https://doi.org/10.1016/j.bmc.2005.03.011.

[39] P.V. Bharatam, D.S. Patel, P. Iqbal, Pharmacophoric features of biguanide derivatives: an electronic and structural analysis, J. Med. Chem. 48 (2005) 7615–7622, https://doi.org/10.1021/jm050602z.

[40] C.K. Jaladanki, A. Gahlawat, G. Rathod, H. Sandhu, K. Jahan, P.V. Bharatam, Mechanistic studies on the drug metabolism and toxicity originating from cytochromes P450, Drug Metab. Rev. 52 (2020) 1–29, https://doi.org/10.1080/03602532.2020.1765792.

[41] N. Taxak, P.V. Bharatam, An insight into the concept and details of mechanism-based inhibition of CYP450, Curr. Res. Pharm. Sci. 11 (2011) 62–67.

[42] N. Taxak, S. Kalra, P.V. Bharatam, Mechanism-based inactivation of cytochromes by furan epoxide: unraveling the molecular mechanism, Inorg. Chem. 52 (2013) 13496–13508, https://doi.org/10.1021/ic401907k.

[43] M. Ramesh, P.V. Bharatam, Importance of hydrophobic parameters in identifying appropriate pose of CYP substrates in cytochromes, Eur. J. Med. Chem. 71 (2014) 15–23, https://doi.org/10.1016/j.ejmech.2013.10.023.

[44] M. Arfeen, D.S. Patel, S. Abbat, N. Taxak, Importance of cytochromes in cyclization reactions: quantum chemical study on a model reaction of proguanil to cycloguanil, J. Comput. Chem. 35 (2014) 2047–2055, https://doi.org/10.1002/jcc.23719.

[45] C.K. Jaladanki, N. Taxak, R.A. Varikoti, P.V. Bharatam, Toxicity originating from thiophene containing drugs: exploring the mechanism using quantum chemical methods, Chem. Res. Toxicol. 28 (2015) 2364–2376, https://doi.org/10.1021/acs.chemrestox.5b00364.

[46] D.K. Singh, A. Sahu, A.A. Wani, P.V. Bharatam, A.K. Chakraborti, S. Giri, S. Singh, Characterization of photodegradation products of bepotastine besilate and *In Silico* evaluation of their physicochemical, absorption, distribution, metabolism, excretion and toxicity properties, J. Pharm. Sci. 109 (2020) 1883–1895, https://doi.org/10.1016/j.xphs.2020.03.004.

[47] C.K. Jaladanki, S. Khatun, H. Gohlke, P.V. Bharatam, Reactive metabolites from thiazole-containing drugs: quantum chemical insights into biotransformation and toxicity, Chem. Res. Toxicol. 34 (2021) 1503–1517, https://doi.org/10.1021/acs.chemrestox.0c00450.

[48] D. Becker, P.V. Bharatam, H. Gohlke, F/G region rigidity is inversely correlated to substrate promiscuity of human cyp isoforms involved in metabolism, J. Chem. Inf. Model. 61 (2021) 4023–4030, https://doi.org/10.1021/acs.jcim.1c00558.

[49] N. Taxak, V. Parmar, D.S. Patel, A. Kotasthane, P.V. Bharatam, *S*-Oxidation of thiazolidinedione with hydrogen peroxide, peroxynitrous acid, and C4a-hydroperoxyflavin: a theoretical study, J. Phys. Chem. A 115 (2011) 891–898, https://doi.org/10.1021/jp109935k.

[50] N. Taxak, V.A. Dixit, P.V. Bharatam, Density functional study on the cytochrome-mediated *S*-Oxidation: identification of crucial reactive intermediate on the metabolic path of thiazolidinediones, J. Phys. Chem. A 116 (2012) 10441–10450, https://doi.org/10.1021/jp308023g.

[51] N. Taxak, P.V. Desai, B. Patel, M. Mohutsky, V.J. Klimkowski, V. Gombar, P. V. Bharatam, Metabolic-intermediate complex formation with cytochrome P450: Theoretical studies in elucidating the reaction pathway for the generation of

reactive nitroso intermediate, J. Comput. Chem. 33 (2012) 1740–1747, https://doi.org/10.1002/jcc.23008.
[52] N. Taxak, P.V. Bharatam, Drug metabolism: A fascinating link between chemistry and biology, Resonance 19 (2014) 259–282, https://doi.org/10.1007/s12045-014-0031-0.
[53] S. Kapoor, G. Dubey, S. Khatun, P.V. Bharatam, Remdesivir: mechanism of metabolic conversion from prodrug to drug, Curr. Drug Metab. 23 (2022) 73–81, https://doi.org/10.2174/1389200223666211228160314.
[54] P.V. Bharatam, S. Khanna, Rapid racemization in thiazolidinediones: a quantum chemical study, J. Phys. Chem. A 108 (2004) 3784–3788, https://doi.org/10.1021/jp0366522.
[55] V.A. Dixit, P.V. Bharatam, Toxic metabolite formation from troglitazone (TGZ): new insights from a DFT Study, Chem. Res. Toxicol. 24 (2011) 1113–1122, https://doi.org/10.1021/tx200110h.
[56] D.S. Patel, M. Ramesh, P.V. Bharatam, CytochromeP450 isoenzyme specificity in the metabolism of anti-malarial biguanides: molecular docking and molecular dynamics analyses, Med. Chem. Res. 21 (2012) 4274–4289, https://doi.org/10.1007/s00044-011-9966-9.
[57] M. Ramesh, P.V. Bharatam, CYP isoform specificity toward drug metabolism: analysis using common feature hypothesis, J. Mol. Model. 18 (2012) 709–720, https://doi.org/10.1007/s00894-011-1105-5.
[58] N. Taxak, K.C. Prasad, P.V. Bharatam, Mechanistic insights into the bioactivation of phenacetin to reactive metabolites: a DFT study, Comput. Theor. Chem. 1007 (2013) 48–56, https://doi.org/10.1016/j.comptc.2012.11.018.
[59] N. Taxak, B. Patel, P.V. Bharatam, Carbene generation by cytochromes and electronic structure of heme-iron-porphyrin-carbene complex: a quantum chemical study, Inorg. Chem. 52 (2013) 5097–5109, https://doi.org/10.1021/ic400010d.
[60] Frisch, M. J.; Trucks, G. W.; Schlegel, H. B.; Scuseria, G. E.; Robb, M. A.; Cheeseman, J. R.; Scalmani, G.; Barone, V.; Petersson, G. A.; Nakatsuji, H.; Li, X.; Caricato, M.; Marenich, A. V.; Bloino, J.; Janesko, B. G.; Gomperts, R.; Mennucci, B.; Hratchian, H. P.; Ortiz, J. V.; Izmaylov, A. F.; Sonnenberg, J. L.; Williams-Young, D.; Ding, F.; Lipparini, F.; Egidi, F.; Goings, J.; Peng, B.; Petrone, A.; Henderson, T.; Ranasinghe, D.; Zakrzewski, V. G.; Gao, J.; Rega, N.; Zheng, G.; Liang, W.; Hada, M.; Ehara, M.; Toyota, K.; Fukuda, R.; Hasegawa, J.; Ishida, M.; Nakajima, T.; Honda, Y.; Kitao, O.; Nakai, H.; Vreven, T.; Throssell, K.; Montgomery, Jr., J. A.; Peralta, J. E.; Ogliaro, F.; Bearpark, M. J.; Heyd, J. J.; Brothers, E. N.; Kudin, K. N.; Staroverov, V. N.; Keith, T. A.; Kobayashi, R.; Normand, J.; Raghavachari, K.; Rendell, A. P.; Burant, J. C.; Iyengar, S. S.; Tomasi, J.; Cossi, M.; Millam, J. M.; Klene, M.; Adamo, C.; Cammi, R.; Ochterski, J. W.; Martin, R. L.; Morokuma, K.; Farkas, O.; Foresman, J. B.; Fox, D. J. Gaussian 16 Rev. C.01, Wallingford, CT, 2016.
[61] Y. Zhao, D.G. Truhlar, The M06 Suite of density functionals for main group thermochemistry, thermochemical kinetics, noncovalent interactions, excited states, and transition elements: two new functionals and systematic testing of four M06-class functionals and 12 other functionals, Theor. Chem. Acc. 120 (2008) 215–241, https://doi.org/10.1007/s00214-007-0310-x.
[62] J. Padmanabhan, R. Parthasarathi, M. Elango, V. Subramanian, B. S. Krishnamoorthy, S. Gutierrez-Oliva, A. Toro-Labbé, D.R. Roy, P.K. Chattaraj, Multiphilic descriptor for chemical reactivity and selectivity, J. Phys. Chem. A 111 (2007) 9130–9138, https://doi.org/10.1021/jp0718909.
[63] V.S. Bryantsev, M.S. Diallo, A.C. Van Duin, W.A. Goddard III, Evaluation of B3LYP, X3LYP, and M06-class density functionals for predicting the binding energies of neutral, protonated, and deprotonated water clusters, J. Chem. Theory Comput. 5 (2009) 1016–1026, https://doi.org/10.1021/ct800549f.
[64] M. Walker, A.J. Harvey, A. Sen, C.E. Dessent, Performance of M06, M06–2X, and M06-HF density functionals for conformationally flexible anionic clusters: M06 functionals perform better than B3LYP for a model system with dispersion and ionic hydrogen-bonding interactions, J. Phys. Chem. A 117 (2013) (2013) 12590–12600, https://doi.org/10.1021/jp408166m.
[65] D. Coskun, S.V. Jerome, R.A. Friesner, Evaluation of the performance of the B3LYP, PBE0, and M06 DFT functionals, and DBLOC-corrected versions, in the calculation of redox potentials and spin splittings for transition metal containing systems, J. Chem. Theory Comput. 12 (2016) 1121–1128, https://doi.org/10.1021/acs.jctc.5b00782.
[66] K. Naelapää, J. van de Streek, J. Rantanen, A.D. Bond, Complementing high-throughput X-Ray powder diffraction data with quantum-chemical calculations: application to piroxicam form III, J. Pharm. Sci. 101 (2012) 4214–4219, https://doi.org/10.1002/jps.23287.
[67] S. Suresh, S. Gunasekaran, S. Srinivasan, Vibrational Spectra (FT-IR, FT-Raman), frontier molecular orbital, first hyperpolarizability, NBO analysis and thermodynamics properties of Piroxicam by HF and DFT methods, Spectrochim. Acta Part a: Mol. Biomol. Spectrosc. 138 (2015) 447–459, https://doi.org/10.1016/j.saa.2014.11.040.
[68] F. Vrečer, M. Vrbinc, A. Meden, Characterization of piroxicam crystal modifications, Int. J. Pharm. 256 (2003) 3–15, https://doi.org/10.1016/s0378-5173(03)00057-7.
[69] P. Panzade, G. Shendarkar, S. Shaikh, P.B. Rathi, Pharmaceutical Cocrystal of Piroxicam: Design, Formulation and Evaluation, Adv. Pharm. Bull. 7 (2017) 399–408, https://doi.org/10.15171/apb.2017.048.
[70] D.C. Hobbs, T.M. Twomey, Metabolism of piroxicam by laboratory animals, Drug Metab. Dispos. 9 (1981) 114–118.
[71] I. Klopčič, M.S. Dolenc, Chemicals and drugs forming reactive quinone and quinone imine metabolites, Chem. Res. Toxicol. 32 (2019) 1–34, https://doi.org/10.1021/acs.chemrestox.8b00213.
[72] M.M. Wolfe, D.R. Lichtenstein, G. Singh, Gastrointestinal toxicity of nonsteroidal antiinflammatory drugs, N. Engl. J. Med. 340 (1999) 1888–1899, https://doi.org/10.1056/NEJM199906173402407.
[73] R.S. Obach, A.S. Kalgutkar, T.F. Ryder, G.S. Walker, *In Vitro* metabolism and covalent binding of enol-carboxamide derivatives and anti-inflammatory agents sudoxicam and meloxicam: insights into the hepatotoxicity of sudoxicam, Chem. Res. Toxicol. 21 (2008) 1890–1899, https://doi.org/10.1021/tx800185b.
[74] A.S. Kalgutkar, I. Gardner, R.S. Obach, C.L. Shaffer, E. Callegari, K.R. Henne, A. E. Mutlib, D.K. Dalvie, J.S. Lee, Y. Nakai, J.P. O'Donnell, J. Boer, S.P. Harriman, A comprehensive listing of bioactivation pathways of organic functional groups, Curr. Drug Metab. 6 (2005) 161–225, https://doi.org/10.2174/1389200054021799.
[75] T. Mizutani, K. Suzuki, Relative hepatotoxicity of 2-(substituted phenyl) thiazoles and substituted thiobenzamides in mice: evidence for the involvement of thiobenzamides as ring cleavage metabolites in the hepatotoxicity of 2-phenylthiazoles, Toxicol. Lett. 85 (1996) 101–105, https://doi.org/10.1016/0378-4274(96)03646-6.
[76] T. Mizutani, K. Yoshida, S. Kawazoe, Formation of toxic metabolites from thiabendazole and other thiazoles in mice identification of thioamides as ring cleavage products, Drug Metab. Dispos. 22 (1994) 750–755.
[77] D.K. Dalvie, A.S. Kalgutkar, S.C. Khojasteh-Bakht, R.S. Obach, J.P. O'Donnell, Biotransformation reactions of five-membered aromatic heterocyclic rings, Chem. Res. Toxicol. 15 (2002) 269–299, https://doi.org/10.1021/tx015574b.
[78] Z.Y.S. Zhang, Handbook of Metabolic Pathways of Xenobiotics, John Wiley & Sons: New York 5 (2014) 2166–2168, https://doi.org/10.1002/9781118541203.xen294.
[79] D.A. Barnette, M.A. Schleiff, L.R. Osborn, N. Flynn, M. Matlock, S.J. Swamidass, G. P. Miller, Dual mechanisms suppress meloxicam bioactivation relative to sudoxicam, Toxicology 440 (2020) 152478–152488, https://doi.org/10.1016/j.tox.2020.152478.
[80] D.A. Barnette, M.A. Schleiff, A. Datta, N. Flynn, S.J. Swamidass, G.P. Miller, Meloxicam methyl group determines enzyme specificity for thiazole bioactivation compared to sudoxicam, Toxicol. Lett. 338 (2021) 10–20, https://doi.org/10.1016/j.toxlet.2020.11.015.
[81] G.S. Prasad, K. Srisailam, R.B. Sashidhar, Metabolic inhibition of meloxicam by specific CYP2C9 inhibitors in *Cunninghamella blakesleeana* NCIM 687: in silico and in vitro Studies, Springerplus. 5 (2016) 1–9, https://doi.org/10.1186/s40064-016-1794-4.
[82] C. Chesne, C. Guyomard, A. Guillouzo, J. Schmid, E. Ludwig, T. Sauter, Metabolism of Meloxicam in human liver involves cytochromes P4502C9 and 3A4, Xenobiotica. 28 (1998) 1–13, https://doi.org/10.1080/004982598239704.
[83] N.M. Davies, N.M. Skjodt, Clinical Pharmacokinetics of Meloxicam, Clin. Pharmacokinet. 36 (1999) 115–126.
[84] Y. Pocker, B.P. Ronald, A nuclear magnetic resonance kinetic study of the acid-catalyzed epoxide ring opening of tetramethylethylene oxide, J. Am. Chem. Soc. 100 (1978) 3122–3127, https://doi.org/10.1021/ja00478a027.
[85] W. Hussain, N.M. Craven, Toxic epidermal necrolysis and Stevens-Johnson syndrome, Clin. Med. 5 (2005) 555–558, https://doi.org/10.1186/1750-1172-5-39.
[86] O.G. Nilsen, Clinical pharmacokinetics of tenoxicam, Clin. Pharmacokinet. 26 (1994) 16–43, https://doi.org/10.2165/00003088-199426010-00003.
[87] S. Ichihara, Y. Tsuyuki, H. Tomisawa, H. Fukazawa, N. Nakayama, M. Tateishi, R. Joly, Metabolism of tenoxicam in rats, Xenobiotica. 14 (1984) 727–739, https://doi.org/10.3109/00498258409151471.
[88] J.A. Balfour, A. Fitton, L.B. Barradell, Lornoxicam: a review of its pharmacology and therapeutic potential in the management of painful and inflammatory conditions, Drugs 51 (1996) 639–657, https://doi.org/10.2165/00003495-199651040-00008.
[89] J. Zhang, X. Tan, J. Gao, W. Fan, Y. Gao, S. Qian, Characterization of two polymorphs of lornoxicam, J. Pharm. Pharmacol. 65 (2013) 44–52, https://doi.org/10.1111/j.2042-7158.2012.01573.x.
[90] J. Ho, M.L. Coote, M. Franco-Pérez, R. Gómez-Balderas, First-principles prediction of the pK_as of anti-inflammatory oxicams, J. Phys. Chem. A 114 (2010) 11992–12003, https://doi.org/10.1021/jp107890p.
[91] G. Hitzenberger, S. Radhofer-Welte, F. Takacs, D. Rosenow, Pharmacokinetics of lornoxicam in man, Postgrad. Med. J. 66 (1990) S22–S27.
[92] P. Bonnabry, T. Leemann, P. Dayer, Role of human liver microsomal CYP2C9 in the biotransformation of lornoxicam, Eur. J. Clin. Pharmacol. 49 (1996) 305–308, https://doi.org/10.1007/BF00226332.
[93] S.I. Ankier, A.E. Brimelow, P. Crome, A. Johnston, S.J. Warrington, P. Turner, H. P. Ferber, Chlortenoxicam pharmacokinetics in young and elderly human volunteers, Postgrad. Med. J. 64 (1988) 752–754, https://doi.org/10.1136/pgmj.64.756.752.
[94] J.C. Roujeau, J.C. Guillaume, J.P. Fabre, D. Penso, M.L. Flechet, J.P. Girre, Toxic epidermal necrolysis (lyell syndrome) incidence and drug etiology in France, 1981–1985, Arch. Dermatol. 126 (1990) 37–42, https://doi.org/10.1001/archderm.1990.01670250043005.
[95] T.F. Woolf, A. Black, T. Chang, *In vitro* metabolism of isoxicam by horseradish peroxidase, Xenobiotica 19 (1989) 1369–1377, https://doi.org/10.3109/00498258909043188.
[96] T.F. Woolf, L.L. Radulovic, Oxicams: Metabolic Disposition in Man and Animals, Drug Metab. Rev. 21 (1989) 255–276, https://doi.org/10.3109/03602538909029942.